

3D DEM SIMULATIONS OF A HIGH SHEAR MIXER

Matthew SINNOTT¹ and Paul CLEARY¹

¹ CSIRO Mathematics and Information Sciences, Clayton, Victoria 3169, AUSTRALIA

ABSTRACT

Mixing of granular materials at high shear rates is poorly understood. The particle trajectories are non-trivial due to recirculation regions resulting from the use of mixing impellers. These regions can greatly influence the segregation and mixing of materials.

Three-dimensional simulations using the Discrete Element Method (DEM) have been performed to investigate high shear mixing in a granular bed. A vertical cylindrical mixer was used. Two types of mixing impeller were considered: a vertical rectangular blade and a horizontal bottom disc, each rotating at 100 rpm. Simulations demonstrated that the degree to which the bed is mixed is sensitive to the shape of the impeller. In visually tracing the interchange of particles between different sections of the bed (by colouring the particles according to their initial positions in either quadrants or annuli) we can directly identify radial and angular mixing patterns for each case. Studying the time evolution of the centroid of each colour, together with the mixing rates, helps us quantify and understand the mixing further.

NOMENCLATURE

C	damping coefficient
F_n	normal collisional force
F_t	tangential collisional force
g	gravitational constant
k	spring constant
R	radius of mixer shell
Δx	particle overlap
ε	coefficient of restitution
η	coefficient of variation of particle colour index
μ	coefficient of friction
v_n	normal velocity
v_t	tangential velocity
ω_D	angular velocity of rigid body

INTRODUCTION

Powder mixing is a fundamental operation for many industries including pharmaceuticals and food processing. The quality of the product depends on the degree of mixing of the constituent materials. However, the homogeneity of the final mixture relies on the nature of the applied mixing procedure. Any systematic mixing process is incapable of creating a completely random mixture since the likelihood of it reordering the particle bed increases with the degree of mixing. Thus there always occurs an equilibrium point where there is a natural cessation of mixing. For stirred mixers, this depends on both the design and operating conditions of the impeller. Unfortunately, due to a lack of understanding of the interaction between the impeller and the granular

material, limited progress has been made in impeller design. Significant research into understanding complex flows near blade impellers has been undertaken by Stewart et al. (2001) and Zhou et al. (2002).

The Discrete Element Method has been used by Kuo et al. (2002) to study mixing. They compared the action of blade and disc impellers with DEM simulations and PEPT data at high shear rates. However, their results for the blade impeller showed particles levitating to the top of the mixer in a highly non-physical manner. This was interpreted as due to a lack of kinetic energy dissipation when using low spring constants. However, this phenomenon was still present for reasonable values of spring constant near 10^7 N/m. We extend their work here using our own DEM simulations under similar conditions to investigate radial and angular flow patterns and mixing rates.

NUMERICAL MODEL

Discrete Element Method

DEM is a particle-based technique. Each particle in the flow is tracked and all collisions between particles and between particles and boundaries are modelled. The contact force law used here is a linear spring-dashpot model where particles are allowed to overlap. The maximum overlap is fixed by the stiffness of the spring, k , which provides a repulsive force. The dashpot contributes the inelastic component of the collision. Its damping coefficient, C , determines the effective coefficient of restitution for the material properties of the granular media. The spring and dashpot together define the normal force.

$$F_n = -k\Delta x + Cv_n \quad (1)$$

In the same way, the tangential force under the sliding friction limit is

$$F_t = \min\left(\mu F_n, \int kv_t dt + Cv_t\right) \quad (2)$$

A general review of DEM and its variants can be found in Barker (1994). The algorithm for the simulation procedure developed and used at CSIRO Mathematical and Information Sciences is as follows:

- (1) A search grid regularly maintains a near-neighbour interaction list for all particle pairs that might suffer a collision in that given period. Boundary objects are described as virtual DEM particles simplifying the treatment of collisions.
- (2) The near-neighbour list is used with the interaction model described above to identify and record all collisions involving particles and boundary particles.

The forces on particle pairs and boundaries are evaluated.

- (3) All forces are summed and define equations of motion for the particle system. These are integrated over a time suitable to resolve each collision.

This has been used to model various industrial granular flows (see Cleary, 2003 and Cleary & Sawley, 2002).

Characterising Mixing

Two methods for predicting mixing and segregation in granular systems have previously been described (Cleary et al. 1998, and Cleary, 1998). The first involves following the position of the centroid for each discrete class of particles (originally used by Metcalfe et al., 1995). When particles from spatially distinct classes intermingle in a rotating geometry, the centroid locations oscillate with an exponentially decaying envelope. The oscillation period and decay rate completely characterise the mixing.

The alternative method is more flexible and can be used with both continuous and discrete particle distributions. A three dimensional grid is constructed over the particles. Local averages of a selected property (eg mass, density, diameter, colour) are calculated using all particles in the region centred at each grid point. These local averages thus define the probability distribution for the chosen property. The mean, standard deviation, and coefficient of variation, η , (defined as mean divided by standard deviation) are calculated for the entire distribution at each time step. Ideal limits are calculated for the coefficient of variation for the fully segregated and fully mixed states, η_s and η_r , respectively. Since the coefficient of variation evolves with time (reflecting mixing and segregation processes in the bed) it is not only a good indicator of the quality of the mixture but also a natural measure of the mixing rate. This mixing/segregation measurement process is described in more detail in Cleary (1998).

SIMULATIONS

Description of Mixer Setup

Following Kuo et al. (2002), the mixer used in the simulations is a vertical cylindrical shell fitted with a disc impeller or a rectangular blade impeller. The dimensions of these components are given in figure 1. No clearance between the impeller and the floor of the mixer shell has been allowed. Solid geometries were built for all mixer components and then meshed with a resolution of 5 mm using the commercial software packages Solidworks and Hypermesh, respectively. Conditions for the simulations were set using a spring constant of 1000 N/m (yielding a collision time step of 9×10^{-6} s). Particle-particle and particle-boundary collisions were both modelled using a coefficient of restitution of 0.9 for reasonably elastic collisions and a particle density of 2500 kg/m^3 . For powder mixing, it is not obvious that generalised material properties are meaningful for the boundaries and particles. Stewart et al. (2001) found the structure of particle flows was relatively insensitive to coefficients of friction in the range 0.3 – 0.5. A coefficient of dynamic friction of 0.4 was chosen for both particle-particle and particle-boundary interactions. Particle diameters ranged from 1.45 to 1.55 mm in order to model the slight variation in particle sizes expected in any real marble assembly.

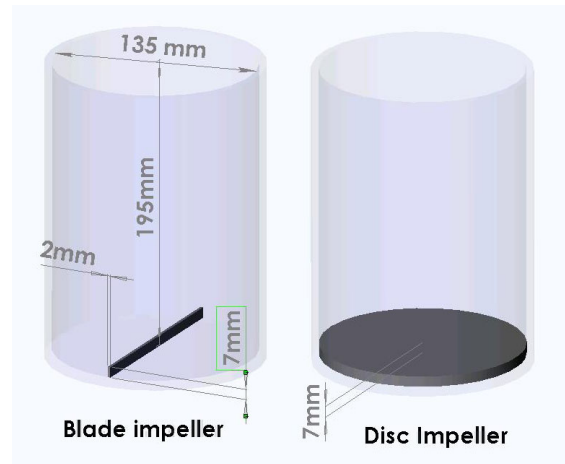


Figure 1: Diagram of mixer geometries fitted with the blade and disc impellers.

Filling the Mixer

For each impeller configuration, the mixer was filled to a bed depth of 25 mm with non-overlapping, near mono-size, spherical particles. These particles were then allowed to gravitationally settle for 1 s. The impellers were set in motion in an anticlockwise direction with a rotation rate of 100 rpm. These were allowed to turn two full revolutions to allow the periodic motion of the bed surface to stabilise. Simulations were then suspended and the particles re-coloured by their position into four distinct particle groups, either as quadrants or as annular rings. This resulted in four simulations with two sets of particle groups for each impeller configuration. The different spatial colouring of these particles lets us make use of the rotational symmetry of the problem to study the mixing regimes in radial and circumferential directions independently. The duration of these simulations was 8 s (~13 revs).

RESULTS

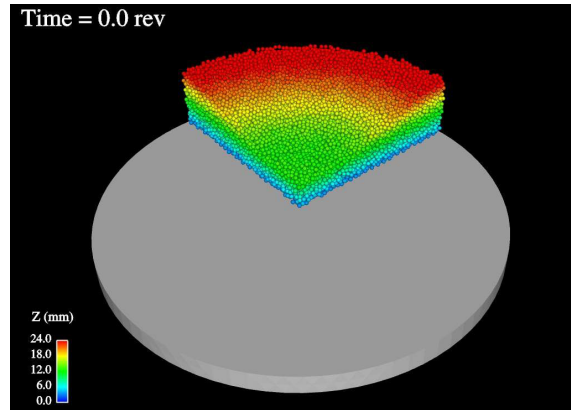
Flow Patterns

Disc Impeller

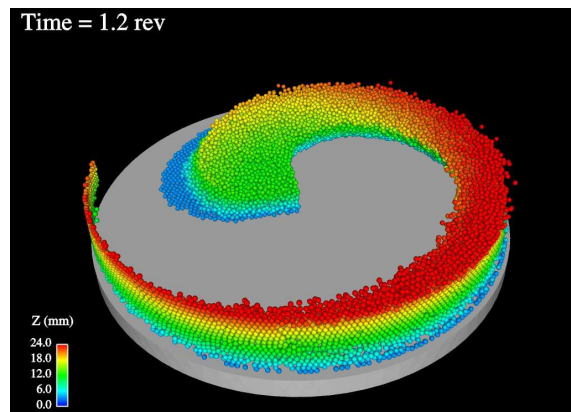
Mixing patterns for the particle quadrants in the simulation involving the disc impeller show simple flow behaviour. A single quadrant is displayed in figure 2 for various times during the mixing process. The other quadrants are present but not visible. Particles are coloured by their height in the bed with blue particles in the lowest layer adjacent to the disc and red particles in the surface of the heap formed near the wall due to centrifugal forces. The motion of the particle bed is driven by the rotation of the disc. Particles near the wall experience a drag force due to particle-wall friction. The central core of the bed is observed to rotate as a rigid body and the outer bands continue to wrap around this central region in a vortex pattern.

These spiralling bands of material are spatially distinct entities and no significant radial mixing occurs between them or with bands in the neighbouring quadrants. This is more evident in figure 3. Here particles have been divided into annular regions and coloured respectively. After 8 s (13.4 rev), almost no exchange of particles has occurred between these groups signifying that no radial mixing results from the action of the disc impeller on the bed.

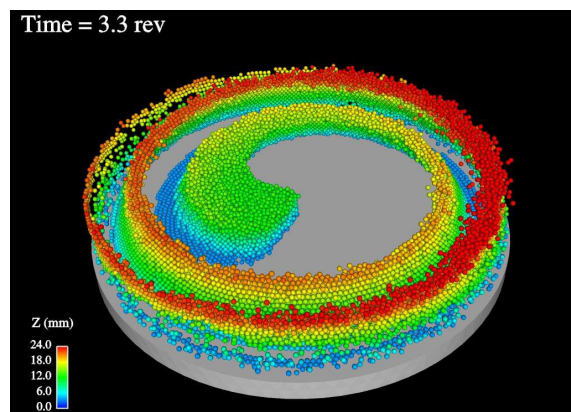
This is due to the fact that a steady state condition has been reached, with the radially compacted bed (particularly the heap formed near the wall) opposing the inertial forces pushing outward towards the wall. Therefore, the only direction that the bed can experience shear is in the direction of rotation. This leads to cumulative strain of the bed by the wall thus preventing the powder from rotating fully as a rigid body.



(a)



(b)



(c)

Figure 2: Snapshots of the mixing of a single quadrant by the disc impeller at various times. Particles are coloured by height in order to clearly visualise the lateral and vertical dispersion of the bed.

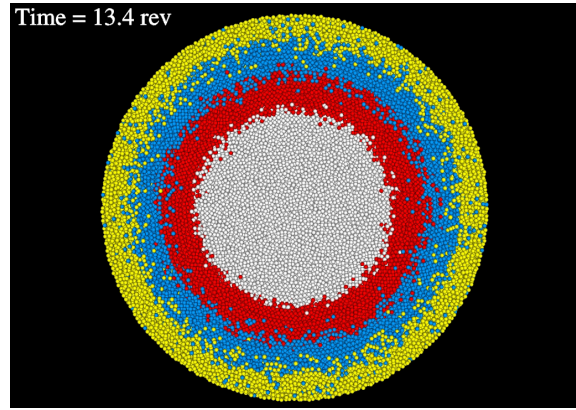


Figure 3: Top view of four annular regions showing the lack of radial mixing in the bed after 8 s.

The average angular velocity of the particles was determined as a function of radial position for the disc impeller and is plotted in figure 4. The dashed line represents the powder mechanics analytical solution of Knight et al. (2001) for this system. They assumed rigid body motion for the powder, deriving an expression for constant angular velocity.

$$\omega_D = \sqrt{\frac{7g}{9R}} \quad (3)$$

The fluctuations seen near the centre of the bed are due to data sparsity. The bed rotates as a rigid body with an angular velocity of ω_D out to approximately half the mixer radius. Near the wall, frictional forces from the container wall dominate and the angular velocity of particles is reduced substantially. This leads to cumulative shear strain, which is the sole mechanism for mixing with this impeller.

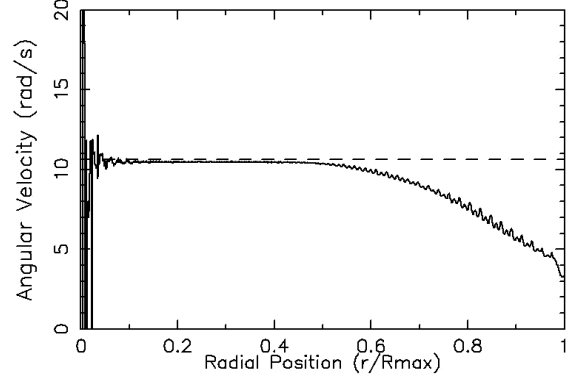


Figure 4: Predicted average angular velocity versus normalised radial position for particles in the disc impeller simulations.

Blade Impeller

Flow behaviour for the blade impeller is more complex. No evidence of the non-physical particle motion observed by Kuo et al. (2002) was evident here. As figure 5(a) shows, particles are pushed gently up into a heap in front of the approaching blade. The blade sweeps through each quadrant initially setting up three distinct vertical layers (at least for the outer radial region of the bed). Particles flowing over the blade are deposited in the void left in the wake of the impeller and fall to the floor of the mixer.

There reaches a point where particles from the next quadrant begin to accumulate in a vertical layer above those of the preceding quadrant. These layers are laterally displaced due to the shearing action of the impeller. This is evident in figure 5(b).

Particles near the surface of the fast moving heap continue to surf down the front of this incline and can remain trapped in recirculation zones there for a considerable time. This results in large lateral dispersion of the surface of each quadrant. By figure 5(c), particles at the bottom of the mixer have been pushed in front of the blade all the way around to the next blade further enhancing the displacement of the vertical layers.

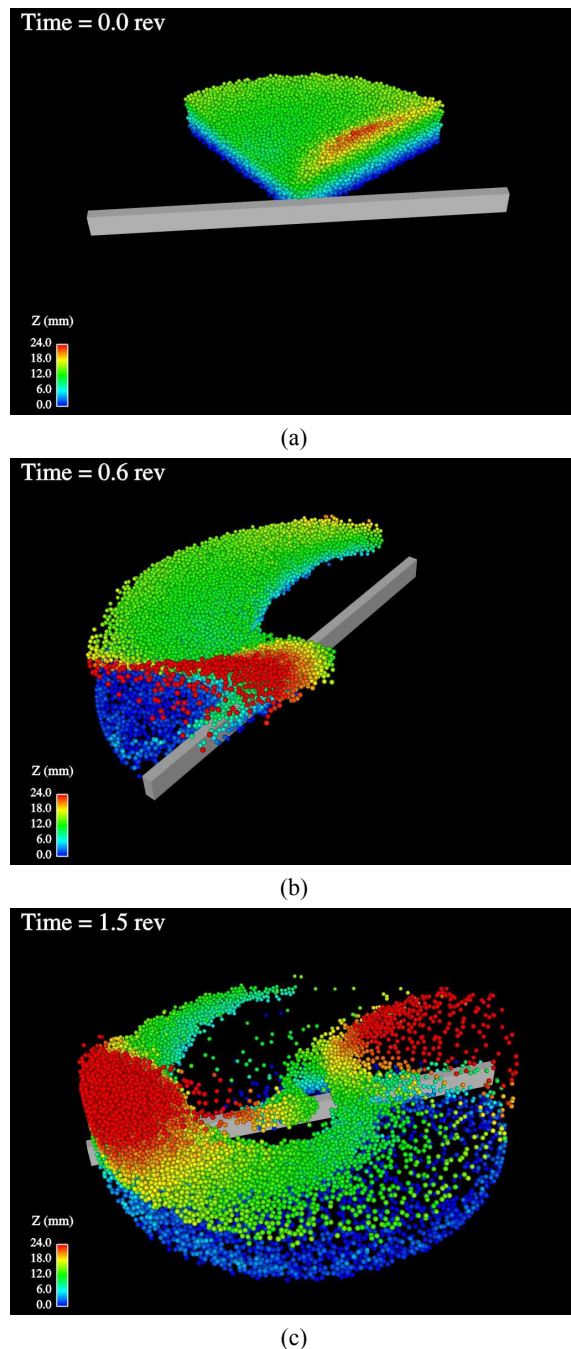


Figure 5: Snapshots of the mixing of a single quadrant by the blade impeller at various times. Particles are coloured by height to observe motion in the top and bottom layers.

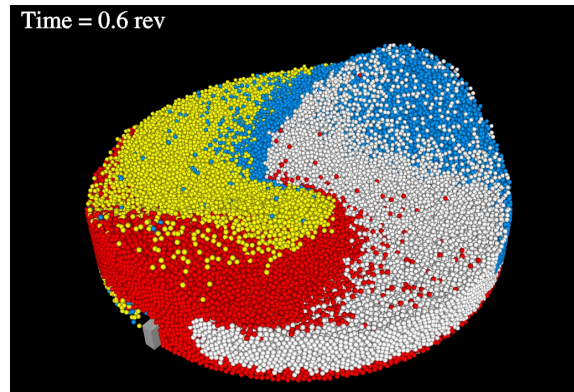


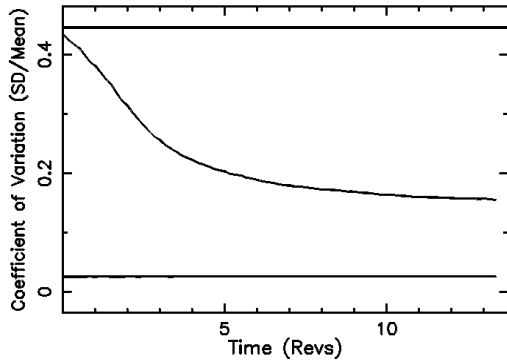
Figure 6: Mixing of the four particle quadrants for the blade impeller at the same time as figure 5(b).

To better observe the presence of these layers, figure 6 shows all four quadrants visible at the same instant of time as that in figure 5(b). These four quadrants are coloured yellow, red, white and blue respectively as a visual aid to the mixing. The layer of red particles visible beneath the bulk of the white quadrant is the result of a previous blade pass. This bottom layer is still relatively unmixed with the white particles. Subsequent blade crossings will begin to mix across this boundary as particles flow over the blade. At the same time, red particles have been spread across the white quadrant in a thin layer. Behind the blade there is a radial surface flow down the heap toward the centre of the mixer. The action of the blade is such that surface particles in front of the heap are thrown radially outward diffusing the already thin surface layer near the walls. Mixing continues rapidly in these top and bottom layers.

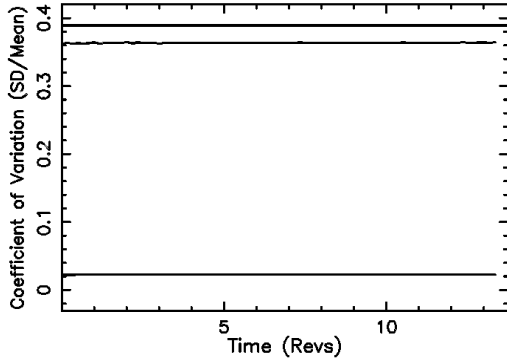
Mixing Rates

The quantitative measures described earlier are used to identify timescales for mixing. The evolution of the coefficient of variation with time is shown in figure 7, for each configuration. Each curve is plotted between the fully non-mixed and fully mixed limits for comparison. Figure 7(a) shows good circumferential mixing for the disc impeller with most of the mixing completed within five revolutions. The curve shows an exponentially decreasing mixing rate with time. As the bed becomes less homogeneous, the number of possible states resulting in further mixing decreases. The likelihood that mixing might result in reordering of the material thus increases. Interestingly, there appears to be no significant radial mixing at all (see figure 7(b)) for the disc impeller. As previously mentioned, this is likely to be due to the lack of shear in the radial direction needed to generate radial migration.

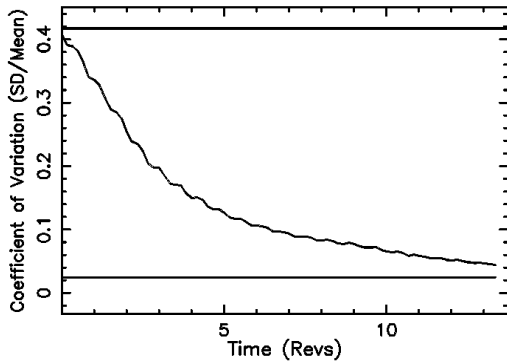
The shape of the curves in figures 7(a) and (c) suggest that for circumferential mixing with both the blade and the disc, the likelihood of further mixing is systematically reduced resulting in the observed exponential decrease with time. However, this rate of mixing is far quicker for the paddle, which has lead to almost complete circumferential mixing in only 13 revolutions. Mixing of the annular regions using the blade shows that there is strong and steady radial mixing (see figure 7(d)) at a slower rate than the initial circumferential mixing. The lack of radial transport of particles when using the disc impeller marks the greatest difference in the mechanism driving the mixing in each configuration.



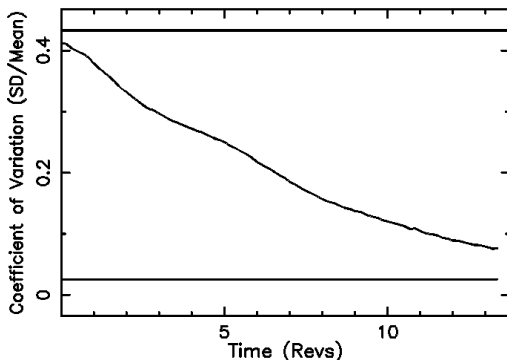
(a)



(b)



(c)



(d)

Figure 7: Coefficient of variation as a function of time for: (a) quadrant for a disc impeller (b) annular mixing for a disc impeller; (c) quadrant for a blade impeller and (d) annular mixing for a blade impeller. Fully non-mixed and mixed limits are shown at top and bottom respectively.

	Disc (quad)	Disc (annuli)	Blade (quad)	Blade (annuli)
Amount of Mixed	65%	7%	87%	75%

Table 1: The amount of mixed material left after 13 revs.

Superimposed on the mixing measures for the blade mixer (see figure 17(c)) are small regular oscillations due to the passage of the blade. The frequency is 2.5 Hz, which is between 1 and 2 times the blade rotation rate. This suggests that the bulk circulation rate of the particles is less than the blade speed due to the retarding effects of the walls. Vertical mixing rates are not shown here, but the mixing can be seen in figures 2 and 5. For the disc, the vertical structure of the flow patterns does not change greatly whereas the paddle initiates significant vertical restructuring of the bed leading to a greater degree of mixing.

The percentage of material mixed after 13 revs for each of the cases is given in table 1. The blade impeller is clearly a much more efficient mixing tool in both circumferential and radial directions.

Time-dependent mixing rates were calculated for each simulation (by taking the gradient of the mixing state). The circumferential mixing rates for both impellers are compared in figure 8. The shape of both curves is very similar. A linear increase in mixing rate occurs up until about two or three revolutions. This is the amount of time required for significant material in each quadrant to travel the circumference of the mixer shell and begin blending with itself again. Following this an exponential decrease in mixing rate occurs with time as further mixing becomes more difficult.

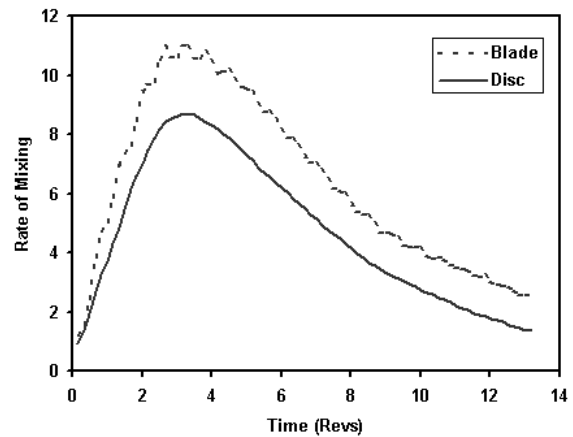


Figure 8: Mixing rates for particle quadrants using the blade and disc impellers.

A further indicator of the kinetics of mixing is the motion of the centroid of each particle group. The radial position of the quadrant centroids (scaled by the particle diameter) is shown in figure 9 for the disc and blade cases. The disc impeller causes a rapid movement of the centroid towards the centre of the mixer in just over one revolution (see figure 9(a)). However, this is simply due to fast mixing of the outer radial layers as seen already in figure 2. The rigid motion of particles near the core (preserving the quadrant ordering of the bed) periodically balances the

spatial weighting of the centroid position by the material in the outer layers. This gives rise to oscillations in the centroid. The core eventually mixes and the oscillations decay. The position of the centroid thus gives a false impression of the timescale of mixing in this case. The time dependence of oscillation intensity provides a more reliable measure.

An exponential decrease in radial centroid position is observed for the paddle impeller (see figure 9(b)) up until about five revolutions. The centroid then remains stationary for three revs at about 10% of the mixer radius away from the central core of the bed. This region begins to mix over another five revolutions, leading to a substantially mixed state of the entire bed after 13 revs. This is in agreement with the longer timescale for radial mixing observed in figure 7(d) The sinusoidal oscillation visible in the centroid curves has the same frequency as that already seen in figure 7(c) (representing the bulk periodic flow of the bed).

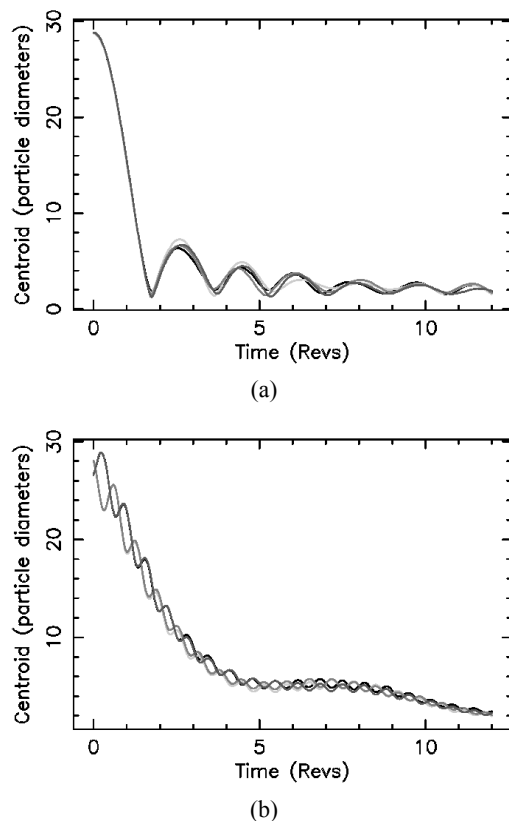


Figure 9: The radial centroid positions for each particle quadrant mixed by (a) the disc impeller and (b) the blade impeller.

CONCLUSION

Flow patterns and mixing rates have been studied for radial and circumferential mixing in rotating impeller high shear mixers using the Discrete Element Method. The blade impeller was shown to be significantly more efficient in mixing the bed than the disc. It has strong mixing in both radial and circumferential directions. No radial mixing was observed for the disc. Further study will be needed to investigate mixing of the vertical layers.

ACKNOWLEDGEMENTS

Due consideration must be given to Prof. J. P. K. Seville for bringing the work of Kuo et al. (2002) to our attention.

REFERENCES

- BARKER, G.C. (1994), "Computer Simulations of Granular Materials", in: A. Mehta (Ed.), *Granular Matter: An Inter-Disciplinary Approach*, Springer, Berlin.
- CLEARY, P.W., METCALFE, G. and LIFFMAN, K. (1998), "How well do discrete element granular flow models capture the essentials of mixing processes?", *Applied Mathematical Modelling* **22**, 995–1008.
- CLEARY, P.W. (1998), "Discrete Element Modelling of Industrial Granular Flow Applications", *TASK. Quarterly – Scientific Bulletin* **2**, 385–416.
- CLEARY, P.W., and SAWLEY, M. (2002), "DEM modelling of industrial granular flows: 3D case studies and the effect of particle shape on hopper discharge", *App. Math. Modelling*, **26**, 89–111.
- CLEARY, P.W. (2003), "Large scale industrial DEM modelling", to appear: *Engineering Computations*.
- KNIGHT, P.C., SEVILLE, J.P.K., WELLM, A.B. and INSTONE, T. (2001), "Prediction of Impeller Torque in High Shear Powder Mixers", *Chemical Engineering Science* **56**, 4457–4471.
- KUO, H.P., KNIGHT, P.C., PARKER, D.J., ADAMS, M.J. and SEVILLE, J.P.K. (2002), "The Stability of Discrete Element Simulations in a High Shear Mixer", *Proceedings of World Congress on Particle Technology* **4**, 21–25 July, Sydney, Australia.
- METCALFE, G., SHINBROT, T., MCCARTHY, J.J. and OTTINO, J.M. (1995), "Avalanche Mixing of Granular Solids", *Nature* **374**, 39–41.
- STEWART, R.L., BRIDGEWATER, J., ZHOU, Y.C. and YU, A.B. (2001), "Simulated and measured flows of granules in a bladed mixer – a detailed comparison", *Chemical Engineering Science* **56**, 5457–5471.
- ZHOU, Y.C., YU, A.B. and BRIDGEWATER, J. (2002), "The effect of blade speed on granular flow in a cylindrical mixer", *Proceedings of World Congress on Particle Technology* **4**, 21–25 July, Sydney.